

RopGEF2 is involved in ABA-suppression of seed germination and post-germination growth of *Arabidopsis*

Shujuan Zhao, Yuxuan Wu, Yuqing He, Yarui Wang, Jun Xiao, Lin Li, Yanping Wang, Xi Chen, Wei Xiong and Yan Wu*
State Key Laboratory of Hybrid Rice, College of Life Sciences, Wuhan University, Wuhan 430072, China

Received 2 June 2015; revised 23 September 2015; accepted 25 September 2015; published online 13 October 2015.

*For correspondence (e-mail wuy@whu.edu.cn).

SUMMARY

The involvement of Rho of Plants (ROP) GTPases in abscisic acid (ABA) signalling in *Arabidopsis* has been demonstrated in many studies. However, the roles of RopGEFs (Rop guanine nucleotide exchange factors), which modulate ROP activities in ABA signalling, are poorly understood. Here, we demonstrate that RopGEF2 may play a negative role in ABA-suppressed seed germination and post-germination growth. We show that disruption of RopGEF2 enhances sensitivity to exogenous ABA in seed germination assays and that RopGEF2pro-GUS is mainly expressed in developing embryos and germinating seeds. Interestingly, YFP-RopGEF2 is located in both the cytoplasmic region and in mitochondria. Notably, the PRONE2 (plant-specific ROP nucleotide exchanger 2) domain of RopGEF2 is detected in mitochondria, whereas the N-terminus of RopGEF2 is shown to be in the cytosol. After ABA treatment, degradation of RopGEF2 is triggered in the cytosol through the ubiquitin-26S proteasome system. The binding of RopGEF2 to ROP2, ROP6 or ROP10, which has been demonstrated to be involved in ABA signalling, not only alters the localization of RopGEF2 but also enables RopGEF2 to escape degradation in the cell. Thus, in this study, we deduce a sophisticated mechanism of ABA-mediated RopGEF2-ROP signalling, which potentially implicates the inactivation of ROPs in responsiveness to ABA.

Keywords: RopGEF2, abscisic acid, seed germination, post-germination growth, ubiquitin-26S proteasome system, mitochondria, *Arabidopsis*.

INTRODUCTION

Abscisic acid (ABA) is essential for many aspects of plant development, ranging from the maturation and germination of seeds to the growth of seedlings and the control of floral transition (Finkelstein *et al.*, 2002; Cutler *et al.*, 2010; Hauser *et al.*, 2011; Wang *et al.*, 2013). The identification of the ABA receptor PYR/PYL/RCAR has enriched our comprehension of the perception and initiation of ABA signalling events (Fujii *et al.*, 2009; Ma *et al.*, 2009; Park *et al.*, 2009; Miyakawa *et al.*, 2013). Although many genes involved in the ABA signalling pathway have been documented in numerous studies (Lopez-Molina *et al.*, 2001; Finkelstein *et al.*, 2002; Raghavendra *et al.*, 2010; Hauser *et al.*, 2011; Wang *et al.*, 2011, 2013), the regulatory mechanisms concerning suppression by ABA of seed germination and post-germination growth are far from fully understood.

Rho of Plants (ROP) GTPases modulate a wide range of developmental processes, including the directional growth of pollen tubes, the establishment of polar root growth and morphogenesis of leaf epidermal cells, as well as responses to phytohormones and environmental signals

(Berken, 2006; Kost, 2008; Yang, 2008; Zhang and McCormick, 2010; Wu *et al.*, 2011, 2013; Craddock *et al.*, 2012; Chang *et al.*, 2013). One of the vital regulators of ROP activity, RopGEFs (Rop guanine nucleotide exchange factors) promote the conversion of ROPs from their inactive GDP-bound form to the active GTP-bound form (Yang, 2002; Shichrur and Yalovsky, 2006). Two groups of RopGEFs are known in animal cells. One is classified on the basis of their conserved DH-PH (Dbl homology-pleckstrin homology) domain and the other contains the DOCK180 (180-kDa protein downstream of CRK) domain (Rossman *et al.*, 2005; Côté and Vuori, 2007). In *Arabidopsis* there are 15 RopGEFs. Fourteen *Arabidopsis* RopGEFs possess PRONE (plant-specific ROP nucleotide exchanger) domains, and one, SPIKE1, contains the DOCK180 domain (Berken *et al.*, 2005; Gu *et al.*, 2006; Basu *et al.*, 2008). The RopGEFs are essential regulators of plant development. Overexpression of *Arabidopsis* RopGEF1 in tobacco pollen induces the depolarization of pollen tube growth. The PRONE1 (DUF315) domain is necessary and sufficient for

the membrane association of RopGEF1 and the activation of ROP1 (Gu *et al.*, 2006). Co-expression of *PRK2a* and *RopGEF12* stimulates isotropic growth of pollen tubes, which mimics the phenotype caused by overexpressing constitutively active (CA) ROP. Unlike PRONE1, the PRONE12 domain of RopGEF12 is not sufficient to induce isotropic pollen tube growth (Zhang and McCormick, 2007). The modulation of ROP11 activity by RopGEF4 is crucial for the initiation of cell wall patterning in xylem cells (Oda and Fukuda, 2012). Roles for RopGEFs in plant hormone signalling have also been reported. RopGEF7 is involved in PLT (PLETHORA)-dependent auxin signalling during root pattern formation (Chen *et al.*, 2011). It has also been determined that RopGEFs are involved in the FER (FERONIA) receptor kinase pathway, which suppresses ABA signalling. The FER-interacting proteins RopGEF1, RopGEF4 and RopGEF10 can activate ROP11. Consequently, activated ROP11 physically interacts with ABI2. Thus, inhibition of ABA signalling by the FER pathway is achieved (Yu *et al.*, 2012). So far, SPIKE1 is the only known DOCK180-related RopGEF in *Arabidopsis*, and it is required for the maintenance of cell shape and for tissue development (Qiu *et al.*, 2002). Although the biological functions of some RopGEFs have been elucidated, the roles of RopGEFs in seed germination and post-germination growth are poorly understood.

Because of the essential roles of ROPs in ABA signalling, modulation of ROP activity is important for regulating ABA signalling (Lemichiez *et al.*, 2001; Li *et al.*, 2001, 2012; Zheng *et al.*, 2002; Yu *et al.*, 2012). Inactivation of ROP2 results in an ABA-hypersensitive response in seed germination in transgenic plants carrying *DN-rop2* (*dominant negative GDP-bound rop2*) (Li *et al.*, 2001). Altered ABA-induced stomatal closure is also reported in transgenic plants expressing *CA-rop6/AtRac1* (*constitutively active GTP-bound rop6/AtRac1*) (Lemichiez *et al.*, 2001). When the function of ROP10 is compromised, enhanced sensitivity to ABA is observed in various circumstances such as in root elongation, seed germination and stomatal closure (Zheng *et al.*, 2002). In addition, ROP11 has been reported to play a negative role in ABA responsiveness (Li *et al.*, 2012; Yu *et al.*, 2012). Clearly, ABA treatment induces the inactivation of ROP GTPases. However, the molecular mechanisms by which ABA controls the activity of ROP remain largely unknown.

To uncover the regulators that control the activity of ROP in the ABA-mediated suppression of seed germination and post-germination growth, we investigated the roles of RopGEF2. We found out that disruption of RopGEF2 led to enhanced sensitivity to ABA during seed germination and post-germination growth. The dynamic and dual localization of RopGEF2 in mitochondria and the cytosol suggests that the spatio-temporal activity pattern of RopGEF2 may be regulated in plant cells in response to ABA. Our findings

that ABA triggered the degradation of RopGEF2 protein in the cytosol via the ubiquitin-26S proteasome system and that RopGEF2 was stabilized by binding to ROP2, ROP6 or ROP10 reveal the complexity of ABA-modulated RopGEF2-ROP signalling in *Arabidopsis*.

RESULTS

Responsiveness to ABA is altered in the *ropgef2-ko* mutant

To investigate the role of *RopGEF2* in the response to ABA, we obtained and characterized the T-DNA insertion mutant *ropgef2-ko* (*SALK_130229*) (Figure 1a). *RopGEF2* expression was completely abolished in *ropgef2-ko* plants, suggesting that *ropgef2-ko* was likely a null mutant (Figure 1b). We compared the seed germination and seedling growth of *ropgef2-ko* with that of wild-type (WT) (*Col-0*) plants grown in various concentrations of ABA (Figure 1c,d). For instance, in the presence of 0.5 μM ABA, 31% of *ropgef2-ko* plants had green cotyledons compared with 61% of WT seedlings (Figure 1d), suggesting that *ropgef2-ko* seedlings were more sensitive to ABA. To further validate the role of *RopGEF2* in the response to ABA, we overexpressed *RopGEF2* in both the *ropgef2-ko* background (*Com* lines) and in the WT background (*OE* lines) (Figure 1b). We scored the cotyledon-greening phenotype for each line in response to different concentrations of ABA (0.3, 0.5 and 1.0 μM) (Figure 1c,d). The reduction in the cotyledon-greening rate was obvious for *ropgef2-ko* treated with 0.3 and 0.5 μM ABA (Figure 1d). Therefore, we further analysed the profiles of seed germination and post-germination growth at 0.5 μM ABA. To compare the phenotypes of each of the tested lines, we carefully measured the kinetics of 'emerged radicles' and 'green cotyledons'. We observed that seed germination (defined as 'emerged radicles') and cotyledon greening were delayed for *ropgef2-ko* (Figure 1e). These results indicated that a lack of *RopGEF2* expression caused hypersensitivity to ABA in seed germination and post-germination growth (Figure 1c–e). We noticed that ABA sensitivity was not obviously affected in radicle emergence and cotyledon greening in transgenic lines overexpressing *RopGEF2* (Figure 1), suggesting that RopGEF2 might exert its function via coupling with its partner(s). Hence, *RopGEF2* overexpression alone might not be sufficient to increase RopGEF2 activity. This effect might be similar to that observed with RopGEF12 (Zhang and McCormick, 2007). In order to stimulate isotropic pollen tube growth the overexpression of both RopGEF12 and its partner AtPRK2a was required (Zhang and McCormick, 2007).

Because only one T-DNA insertion *ropgef2-ko* mutant line was available, we generated artificial microRNA lines with reduced expression levels of *RopGEF2* in the WT background. In total, 47 independent *amiR-RopGEF2* lines

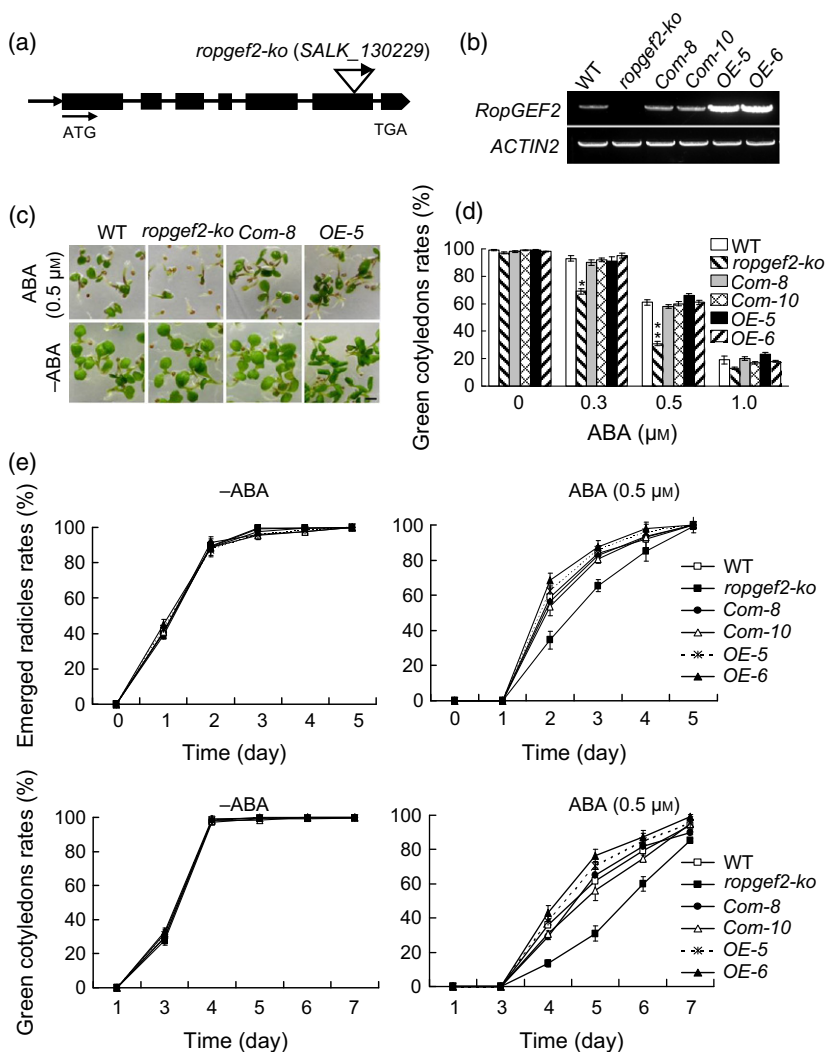


Figure 1. The *ropgef2-ko* mutants showed enhanced sensitivity to ABA during seed germination and post-germination growth.

(a) Schematic diagram (not to scale) indicating the T-DNA insertion in mutant *ropgef2-ko* (SALK_130229). Black boxes and lines indicate exons and introns, respectively, in *RopGEF2*. The promoter region is drawn as an arrow, and the arrowhead indicates the orientation of the T-DNA insert.

(b) Analysis of *RopGEF2* expression in 2-day-old wild-type (WT; Col-0), *ropgef2-ko* and transgenic seedlings expressing p35S-*RopGEF2* in the *ropgef2-ko* (*Com* lines) or WT background (*OE* lines). The expression of *ACTIN2* (*At3G18780*) was used as an internal control.

(c) The enhanced ABA sensitivity of *ropgef2-ko*. Seeds were sown on MS medium without (-ABA) or with ABA (0.5 μM). Photographs were taken on the fifth day after stratification. Scale bar: 0.5 cm.

(d) The green cotyledons rates (%) were scored on the fifth day after stratification. Seeds were sown on MS medium containing ABA (0, 0.3, 0.5 and 1.0 μM). Data represent the mean ± SD of three independent experiments ($n > 70$ for each experiment; * $P < 0.05$; ** $P < 0.01$).

(e) Phenotypes were analysed by measuring the rates of emerged radicle (%) and green cotyledons (%) at the indicated time points (days after stratification). Seeds were sown on MS medium without (-ABA) or with ABA (0.5 μM). Data represent the mean ± SD of three independent experiments ($n > 60$ for each experiment).

were obtained and characterized in the T_1 generation. To determine the specificity of all the selected *amiR-RopGEF2* lines, the expression level of *RopGEF3*, which shares the highest sequence homology to *RopGEF2*, was also examined in parallel. *RopGEF3* expression was not affected in the *amiR-RopGEF2* lines (Figure S1a in the Supporting Information). Ten *amiR-RopGEF2* lines with varying degrees of decreased expression of *RopGEF2* were further analysed (Figure S1a). Six of 10 *amiR-RopGEF2* lines (numbers 1, 2, 4, 6, 7 and 13) showed a reduction in cotyledon greening when grown in 0.3 and 0.5 μM ABA (Figure S1b). Because lines 1 (5.1-fold reduction), 2 (4.3-fold reduction) and 7 (4.8-fold reduction) displayed a strong reduction in *RopGEF2* expression, we chose to compare their radicle emergence and cotyledon greening with the WT, as well as line 10, which had only a 1.4-fold reduction in *RopGEF2* expression (Figure S1a). In the presence of 0.5 μM ABA, a significant delay in radicle emergence and cotyledon greening was observed in *amiR-RopGEF2* lines 1, 2 and 7

but not in line 10 (Figure 2). Collectively, these results demonstrated that the reduced *RopGEF2* expression in the *amiR-RopGEF2* plants may be responsible for the observed delay in seed germination and post-germination growth in the presence of ABA.

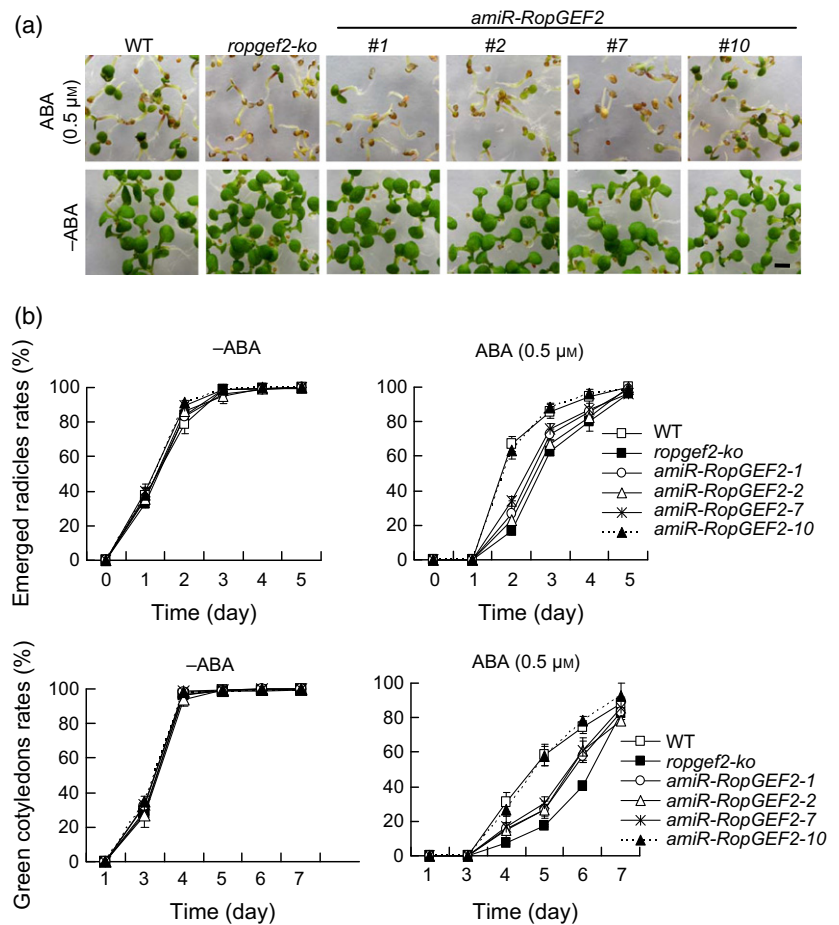
RopGEF2pro-GUS is preferentially expressed in developing embryos and germinating seeds

To better understand the roles of *RopGEF2* in responding to ABA during seed germination and seedling growth, we examined the expression profiles of *RopGEF2* in various *Arabidopsis* tissues. First, the expression pattern of *RopGEF2* was analysed quantitatively. Although *RopGEF2* transcripts were detectable in all tissues tested (e.g. cotyledons, rosette leaves, roots, stems, flowers, siliques, seeds and seedlings), significant levels of expression of *RopGEF2* were detected in siliques and seeds (Figure 3a). To determine the effects of ABA on expression of *RopGEF2* we also measured *RopGEF2* expression in tissues that

Figure 2. The enhanced ABA-sensitivity of the *amiR-RopGEF2* lines during seed germination and post-germination growth.

(a) The *amiR-RopGEF2* lines showed enhanced sensitivity to ABA. Seeds were sown on MS medium without (-ABA) or with ABA (0.5 μM). Photographs were taken on the fifth day after stratification. Scale bar: 0.5 cm.

(b) Phenotypes were analysed by scoring the rate of emerged radicles (%) and green cotyledons (%) at the indicated time points (days after stratification). Seeds were sown on MS medium without (-ABA) or with ABA (0.5 μM). Data represent the mean \pm SD of three independent experiments ($n > 50$ for each experiment).



were treated with ABA (10 μM). Despite treatment with ABA, the level of expression of *RopGEF2* was not significantly affected (Figure 3a), suggesting that ABA might not influence the expression of *RopGEF2* in the tissues tested.

Next, transgenic plants carrying *RopGEF2*pro-GUS were generated and analysed. Abundant GUS signals were observed in developing embryos and mature seeds (Figure 3b1–b4), as well as in germinating seeds and seedlings (Figure 3b5–b11). The *RopGEF2*pro-GUS signal progressively declined during the process of seed germination. Notably, the *RopGEF2*pro-GUS signal was restricted to the meristem and the vascular tissues of leaves and roots at day 5 of germination (Figure 3b11). Thus, the preferential expression patterns of *RopGEF2*pro-GUS in embryos and germinating seeds may suggest a specific function for *RopGEF2* in seed germination and seedling growth.

RopGEF2 is associated with mitochondria

To better understand the function of *RopGEF2*, we characterized the cellular localization of *RopGEF2* in transgenic lines expressing a YFP-*RopGEF2* fusion protein (Figure S2a). The expression of YFP-*RopGEF2* in *ropgef2-ko* plants rescued the phenotype of cotyledon greening

(Figure S2b), demonstrating that the YFP-*RopGEF2* fusion protein was functional. Subsequently, the cellular localization of YFP-*RopGEF2* was analysed in epidermal cells of 5-day-old YFP-*RopGEF2* transgenic seedlings. In addition to localization at the cell periphery, scattered speckles of YFP-*RopGEF2* were also observed in the cytoplasm of epidermal cells in roots and leaves (Figure 4a). To determine the nature of the speckles, we tested several organelle markers, which were transformed individually into the cells of YFP-*RopGEF2* transgenic plants. Our results indicated that YFP-*RopGEF2* co-localized with the mitochondrial marker Mito Tracker Red in protoplasts isolated from YFP-*RopGEF2* transgenic plants (Figure 4b), suggesting a possible mitochondrial localization of YFP-*RopGEF2*. To further clarify the cellular localization of YFP-*RopGEF2*, we analysed cellular fractions by immunoblotting. The YFP-*RopGEF2* fusion protein was detected in purified fractions of membranes (M), cytosol (C) and mitochondria (Mito) (Figure 4c). Furthermore, the cellular localization of YFP-*RopGEF2* was also confirmed via immunofluorescence staining. In this experiment, the signal from AOX1/2 (mitochondrial alternative oxidase isoforms) marks the location of mitochondria. Indeed, YFP-*RopGEF2* and AOX1/2 were

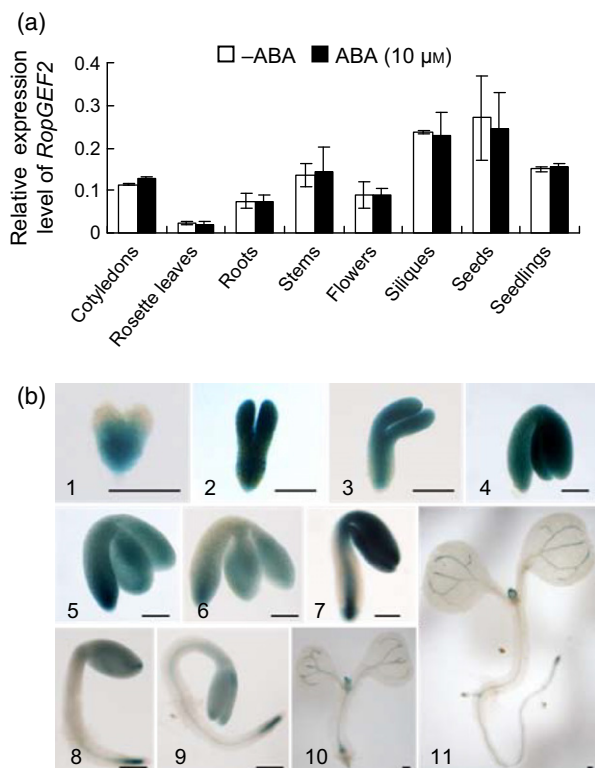


Figure 3. The tissue-specific expression profile of the *RopGEF2* gene. (a) The expression levels of *RopGEF2* were measured in various *Arabidopsis* tissues. The tested *Arabidopsis* tissues were treated with or without ABA (10 μM) for 24 h. *ACTIN2* expression was used as an internal control. Data represent the mean ± SD of three replicates. This experiment was repeated three times ($n = 3$ for each experiment). (b) The expression of *RopGEF2*pro-GUS was detectable in developing embryos and germinating seeds and seedlings (b1, heart-shaped embryo; b2, torpedo-shaped embryo; b3, walking-stick embryo; b4, mature embryo; b5, imbibed seeds for 1 day; b6, imbibed seeds for 2 days; b7–b11, seeds in germination at 1, 2, 3, 4 and 5 days, respectively). Scale bars: 100 μm.

observed to co-localize in root epidermal cells (Figure 4d). Our results suggested that *RopGEF2* associates with mitochondria in the cell.

Full-length *RopGEF2* contains an N-terminal domain (amino acids 1–116) and a PRONE2 (amino acids 117–486) domain (Gu *et al.*, 2006) (Figure 4e). To test the contribution of the N-terminal and PRONE2 domains to the cellular localization of *RopGEF2*, we examined N-terminal and PRONE2 domain truncations using transient expression assays (Figure 4f–h). The p35S-YFP-*RopGEF2*-N or p35S-YFP-PRONE2 plasmid was delivered into *Arabidopsis* leaf epidermal cells using the biolistic bombardment method. The fluorescent signal of YFP-*RopGEF2*-N (N-terminus) appeared in the cytoplasm and cell periphery (Figure 4f). In parallel, scattered speckles of YFP-PRONE2 (PRONE2) were observed in the cell (Figure 4f,g), which resembled the pattern seen in epidermal cells of full-length YFP-*RopGEF2* transgenic plants (Figure 4a,b,d). To distinguish the characteristics of the speckles, we co-transformed the p35S-

YFP-PRONE2 and Mito-DsRed plasmids (for detecting mitochondrial localization) into the epidermal cells of onion peels using the biolistic bombardment method. As shown in Figure 4(h), YFP-PRONE2 and Mito-DsRed were observed to co-localize in the transformed onion epidermal cells (Figure 4h), demonstrating that the PRONE2 domain is crucial for directing *RopGEF2* to mitochondria.

Because PRONE3 shares the highest homology to PRONE2, we also examined the cellular distributions of YFP-*RopGEF3* and YFP-PRONE3. Interestingly, the fluorescent signals of YFP-*RopGEF3* and YFP-PRONE3 were detected near the cell periphery and in the cytosol but not in the mitochondria (Figure S2c). Taken together, these results demonstrate that the distinctive mitochondrial localization of *RopGEF2* might reflect its unique function in *Arabidopsis*.

The cellular localization of *RopGEF2* is altered when it is bound by ROPs

Although numerous studies have reported essential roles for ROP2, *ROP6/AtRac1* and ROP10 in ABA signalling (Lemichez *et al.*, 2001; Li *et al.*, 2001; Zheng *et al.*, 2002), the role of *RopGEFs* in modulating the activity of ROP during the ABA response is poorly understood. Therefore, we decided to investigate the consequences of associating *RopGEF2* with ROPs that are involved in ABA signalling. We showed that *RopGEF2* was able to interact with ROP2, ROP6 and ROP10 (Figure 5a–c). Interestingly, the interaction between *RopGEF2* and ROP2, ROP6 or ROP10 led *RopGEF2* to localize near the cell periphery (Figure 5b), suggesting that binding of ROP alters the localization of *RopGEF2*. To validate this hypothesis, we tagged ROP2, ROP6 or ROP10 with cyan fluorescent protein (CFP) and introduced the tagged constructs into mesophyll protoplasts isolated from YFP-*RopGEF2* transgenic plants. Again, no speckles were observed in the transformed protoplasts. Instead, the fluorescence of YFP-*RopGEF2* was observed in the cytoplasm and cell periphery (Figure S3a). To further test this effect, we generated hybrid lines by crossing YFP-*RopGEF2* transgenic plants to CFP-*ROP2*, CFP-*ROP6*, and CFP-*ROP10* lines. As shown in Figure 5(d), rather than the speckled YFP-*RopGEF2* fluorescent signal, the YFP-*RopGEF2* fluorescent signal was obviously distributed near the cell periphery in all the tested hybrid lines (Figure 5d). Similarly, the speckled YFP-PRONE2 signal was also diminished when co-expressed with CFP-tagged ROP2, ROP6 or ROP10 in onion peel epidermal cells (Figure S3b). Overall, these results suggested that *RopGEF2* translocation in cells might be essential for the modulation of ROP activity.

The PRONE2 domain has no effect on the ABA response during cotyledon greening

To explore the contribution of the PRONE2 domain to the ABA response, we also evaluated the influence of the

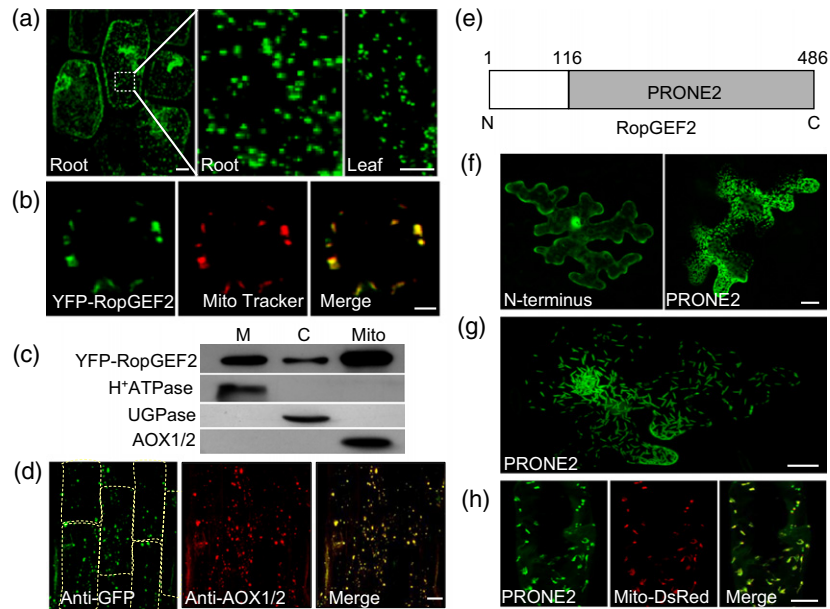


Figure 4. The cellular localization of RopGEF2 and PRONE2.

(a) The cellular localization of RopGEF2 was analysed in the root and leaf epidermal cells of 5-day-old *YFP-RopGEF2* transgenic seedlings. Scale bars: 10 μm . (b) Co-localization of the fluorescent signals from YFP-RopGEF2 and Mito Tracker Red was observed in the mesophyll protoplasts isolated from 5-day-old *YFP-RopGEF2* transgenic seedlings. Mito Tracker Red was used to show mitochondria. Scale bar: 10 μm . (c) Membranes (M), cytosolic (C), and mitochondrial (Mito) protein fractions were purified from 5-day-old *YFP-RopGEF2* transgenic seedlings and analysed by immunoblotting. The purity of each fraction was examined with antibodies detecting the membrane protein H⁺-ATPase, the cytoplasmic isoform of UDP-glucose pyrophosphorylase (UGPase), and the mitochondrial alternative oxidase isoforms (AOX1/2). Anti-GFP antibody was used to detect YFP-RopGEF2. (d) The co-localization (Merge) of YFP-RopGEF2 (Anti-GFP) and AOX1/2 (Anti-AOX1/2) was analysed in root cells of 5-day-old *YFP-RopGEF2* transgenic plants using immunofluorescence staining. Mouse anti-GFP (Anti-GFP) was used to detect YFP-RopGEF2, and rabbit anti-AOX1/2 (Anti-AOX1/2) was used to detect AOX1/2. The secondary antibodies FITC-anti-mouse (green) and Cy3-anti-rabbit (red) were used to detect the Anti-GFP and Anti-AOX1/2 signals, respectively. Scale bars: 10 μm . (e) Schematic diagram (not to scale) showing the N-terminal (amino acids 1–116) and PRONE2 domains (amino acids 117–486) of RopGEF2. Positions of amino acid residues are indicated. (f) The cellular localization of YFP-RopGEF2-N (N-terminus) and YFP-PRONE2 (PRONE2) were analysed in a transient expression assay. Plasmid p35S-YFP-RopGEF2-N or p35S-YFP-PRONE2 was delivered into leaf epidermal cells through the biolistic bombardment method. Scale bar: 10 μm . (g) The cellular localization of YFP-PRONE2 (PRONE2) was analysed in a transient expression assay. Plasmid p35S-YFP-PRONE2 was delivered into leaf epidermal cells through the biolistic bombardment method. Scale bar: 10 μm . (h) The co-localization (Merge) of YFP-PRONE2 domain (green) and Mito-DsRed (red) was analysed in a transient expression assay. Plasmids p35S-YFP-PRONE2 and Mito-DsRed were delivered together into onion peel epidermal cells through the biolistic bombardment method. Scale bar: 30 μm .

PRONE2 domain on cotyledon greening. Transgenic lines expressing the p35S-PRONE2 plasmid in the WT and *ropgef2-ko* backgrounds were generated and characterized (Figure S4a). Interestingly, PRONE2 overexpression in *ropgef2-ko* mutants failed to rescue the cotyledon-greening phenotype (Figure S4b). It is likely that the PRONE2 domain is not sufficient to fulfil the function of RopGEF2 *in planta*. In general, RopGEF-ROPs exert their functions by coupling with downstream effectors. We speculate that the N-terminal domain of RopGEF2 may also play a role in mediating the activation of downstream effectors, at least in the ABA-mediated suppression of seed germination and seedling growth.

ABA stimulates degradation of RopGEF2 via the ubiquitin-26S proteasome system

To investigate how RopGEF2 is affected in response to ABA, we evaluated RopGEF2 expression at the mRNA and protein levels. We found that *RopGEF2* gene expression was not greatly altered by ABA (10 μM) treatment

(Figure 6a). However, levels of RopGEF2 protein were significantly decreased in 5-day-old *YFP-RopGEF2* transgenic seedlings treated for 4 h with various concentrations of ABA (10, 50 and 100 μM) (Figure 6b). Because the reduced RopGEF2 protein level was detectable at 10 μM ABA, we used this concentration to track the kinetics of decline of RopGEF2 over time. Significant decreases in RopGEF2 protein levels were observed within 2 h (120 min) of ABA treatment, and RopGEF2 protein was barely detectable 4 h (240 min) after treatment (Figure 6c). To determine the degradation pathway of RopGEF2 protein triggered by ABA, we examined the effect of proteasome inhibition on the stability of RopGEF2 protein. Prior to the ABA (10 μM) treatment, 5-day-old *YFP-RopGEF2* transgenic seedlings were pre-treated with 50 μM MG132 (26S proteasome inhibitor) for 2 h, and then the level of RopGEF2 protein was examined at various time points. Degradation of RopGEF2 protein was slowed by the addition of MG132 prior to the ABA treatment (Figure 6d). Hence, the contribution of the ubiquitin-26S proteasome system to ABA-induced

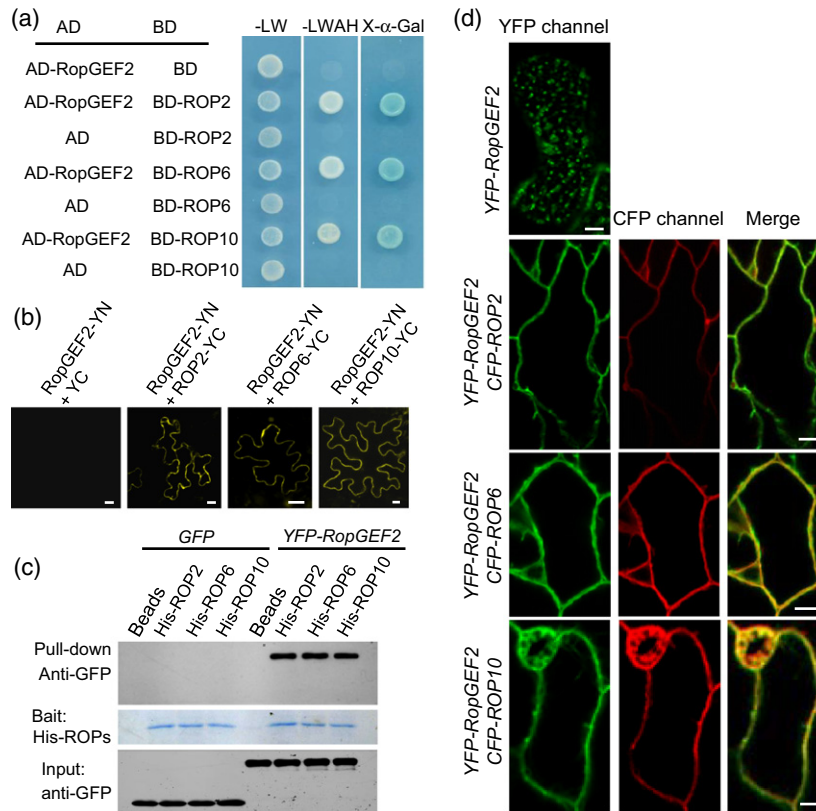


Figure 5. The interaction of RopGEF2 with ROPs was examined *in vivo* and *in vitro*.

(a) The interaction of RopGEF2 with ROP2, ROP6 or ROP10 was analysed using the yeast two-hybrid (Y2H) assay. Empty vectors pGBKT (BD vector) and pGADT (AD vector) were used as controls. -LW, low-stringency medium (SD/Leu⁻/Trp⁻); -LWAH, high-stringency selective medium (SD/Leu⁻/Trp⁻/His⁻/Ade⁻).

(b) The interaction of RopGEF2 with ROP2, ROP6 or ROP10 was analysed using bimolecular fluorescence complementation (BiFC) assay. Plasmids p35S-RopGEF2-YN and p35S-ROP2-YP, p35S-ROP6-YP or p35S-ROP10-YP were delivered into leaf epidermal cells by the biolistic bombardment method. The empty vector p35S-YC (YC, N-terminus of YFP; YC, C-terminus of YFP) was used as a negative control. Scale bars: 10 μm.

(c) The interaction of RopGEF2 with ROP2, ROP6 or ROP10 was analysed using the semi-*in-vivo* protein pull-down assay. Total proteins were extracted from YFP-RopGEF2 transgenic plants and incubated with purified and TALON-bead-conjugated recombinant His-ROPs. After washing, the collected proteins (pellets) were separated via 10% SDS-PAGE and then subjected to immunoblotting with anti-GFP antibody (pull-down). For the controls (Bait), the purified His-ROP proteins were visualized with Coomassie staining. The input total proteins from YFP-RopGEF2 or GFP (empty vector control) transgenic plants were immunoblotted with anti-GFP antibody (Input).

(d) The co-localization of RopGEF2 and ROP2, ROP6 or ROP10 was observed in crossed hybrid lines YFP-RopGEF2 CFP-ROP2, YFP-RopGEF2 CFP-ROP6 and YFP-RopGEF2 CFP-ROP10. Scale bar: 10 μm.

degradation of RopGEF2 was further evaluated. Immunoprecipitation assays were performed to detect the ubiquitination of proteins using a specific anti-ubiquitin antibody. As shown in Figure 6, ABA was indeed able to trigger the ubiquitination of the *Arabidopsis* RopGEF2 protein (Figure 6e,f). We hypothesize that ABA triggers the degradation of RopGEF2 via the ubiquitin–26S proteasome system to attenuate ROP signalling.

To investigate the correlation of RopGEF2 localization and its degradation in response to ABA, we purified and examined membrane (M), cytosolic (C) and mitochondrial (Mito) fractions from YFP-RopGEF2 transgenic seedlings that were treated with or without 10 μM ABA for 4 h. We observed a marked decrease in RopGEF2 protein in the cytosolic (C) fraction. However, detectable levels of RopGEF2 protein remained in the membrane (M) and

mitochondrial (Mito) fractions (Figure 7a). Therefore, ABA-triggered RopGEF2 degradation most likely took place in the cytosol. Because the distribution of RopGEF2 could be altered upon binding to ROP2, ROP6 or ROP10 (Figure 5d), we sought to investigate the correlation between the stability of RopGEF2 and its binding to its target ROPs. To this end, we analysed the behaviour of RopGEF2 protein in YFP-RopGEF2 CFP-ROP2, YFP-RopGEF2 CFP-ROP6 and YFP-RopGEF2 CFP-ROP10 hybrid lines with or without ABA treatment. Notably, the ABA-triggered degradation of RopGEF2 protein was eliminated in seedlings from the hybrid lines (Figure 7b), suggesting that co-expression of RopGEF2 and ROP stabilized the RopGEF2 protein, which was consistent with the phenomena observed for the translocation of YFP-RopGEF2 in the YFP-RopGEF2 CFP-ROP hybrid lines (Figure 5d). These results suggest that the degrada-

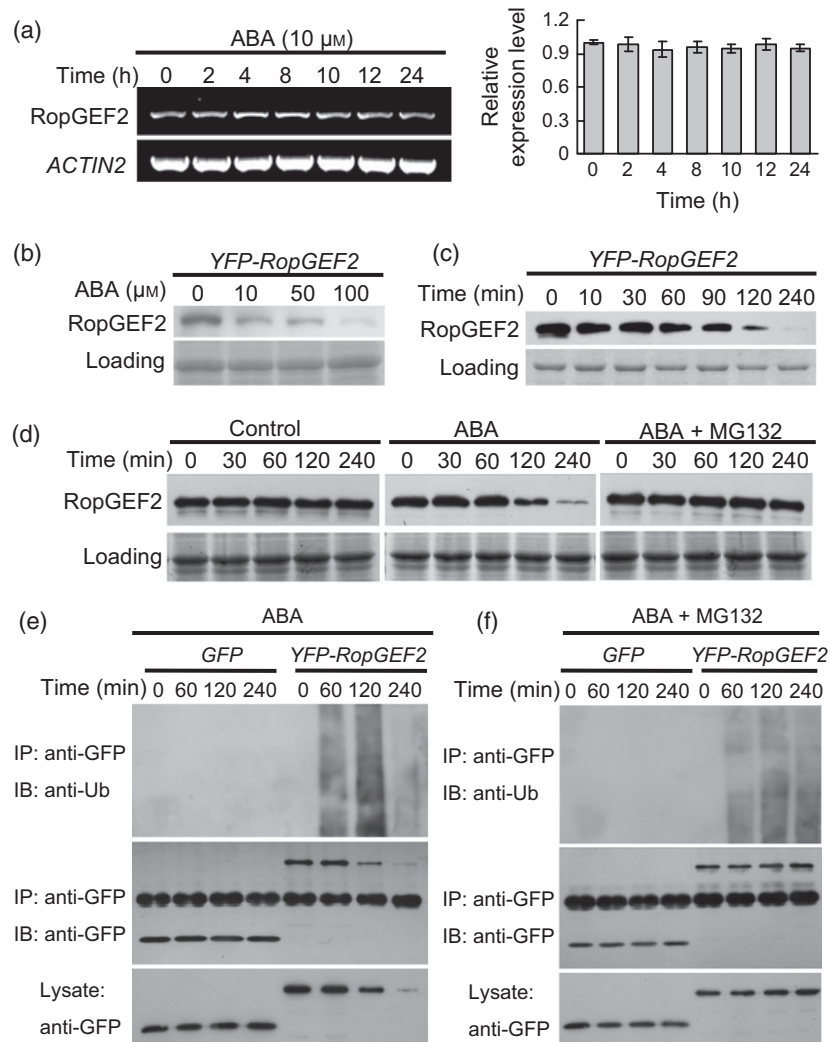


Figure 6. The ABA-induced degradation of RopGEF2 protein.

(a) The *RopGEF2* gene expression profile was examined upon treatment with ABA (10 μM). Total RNA was isolated from 5-day-old wild-type (WT) seedlings treated with 10 μM ABA at the indicated time points (h, hour). *ACTIN2* expression was used as an internal control. The relative expression level of *RopGEF2* was quantified. This experiment was repeated three times ($n = 3$ for each experiment). (b) Five-day-old *YFP-RopGEF2* transgenic seedlings were treated with various concentrations of ABA for 4 h, and then total protein extracts were analysed by immunoblotting with anti-GFP antibody. Coomassie staining of the Rubisco large subunit served as a loading control. (c) Five-day-old *YFP-RopGEF2* transgenic seedlings were treated with 10 μM ABA for the indicated times and were then analysed by immunoblotting. RopGEF2 protein was detected with an anti-GFP antibody. Coomassie staining of the Rubisco large subunit served as a loading control. (d) Treatment with MG132 (26S proteasome inhibitor) blocked the destabilization of RopGEF2 protein induced by ABA treatment. Five-day-old *YFP-RopGEF2* transgenic seedlings were pre-treated with MG132 (50 μM) for 2 h and then treated with ABA (10 μM) for the indicated times. RopGEF2 protein was detected with an anti-GFP antibody. Coomassie staining of the Rubisco large subunit served as a loading control. (e) The ubiquitination of RopGEF2 protein was triggered by ABA treatment. Five-day-old *YFP-RopGEF2* transgenic seedlings were treated with ABA (10 μM) for the indicated times. Total protein was extracted and then immunoprecipitated with anti-GFP antibody. The immunoprecipitated proteins (IP) were denatured and then analysed by immunoblotting (IB) with anti-ubiquitin (Anti-Ub) and anti-GFP antibodies (Anti-GFP). Protein expression (Lysate) was examined by immunoblotting with anti-GFP antibody. (f) The ABA-triggered degradation of RopGEF2 was blocked by MG132. Five-day-old *YFP-RopGEF2* transgenic seedlings were treated with MG132 (50 μM) for 2 h before treatment with ABA (10 μM). Total protein was extracted and then immunoprecipitated with anti-GFP antibody. The immunoprecipitated proteins (IP) were denatured and then analysed by immunoblotting (IB) with anti-ubiquitin (Anti-Ub) and anti-GFP antibody (Anti-GFP). Protein expression (Lysate) was examined by immunoblotting with anti-GFP antibody.

tion of RopGEF2 may be averted when RopGEF2 is bound by its target ROPs, even in the presence of ABA.

DISCUSSION

Modulated by regulators such as RhoGDIs, RopGEFs and RhoGAPs, ROPs are essential molecules for assorted

developmental processes in *Arabidopsis* (Berken, 2006; Kost, 2008; Yang, 2008; Zhang and McCormick, 2010; Wu *et al.*, 2011; Craddock *et al.*, 2012). The RopGEFs are known to be versatile regulators of ROP activity, but the contribution of RopGEFs to the ABA-mediated inhibition of seed germination and post-germination growth is poorly

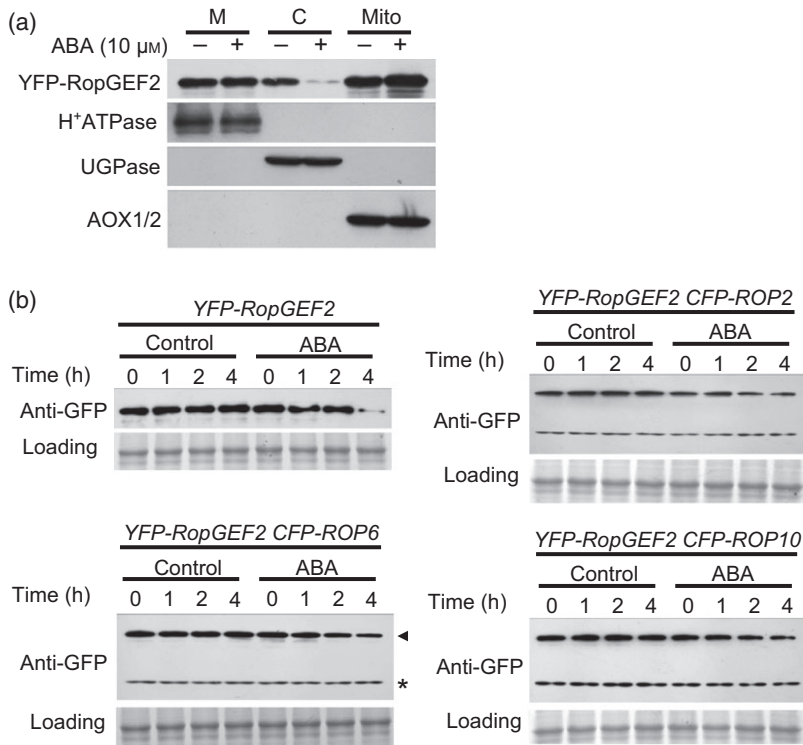


Figure 7. ABA-induced degradation of RopGEF2 was observed in the cytosol, and coexpression of RopGEF2 with ROPs enhanced the stability of RopGEF2.

(a) Observation of ABA-induced degradation of RopGEF2 in the cytosolic fraction. Membranes (M), cytosolic (C) and mitochondrial (Mito) protein fractions were purified from the cells of 5-day-old *YFP-RopGEF2* transgenic seedlings that were treated with or without ABA ($10 \mu\text{M}$) for 4 h. The purity of each fraction was examined using antibodies against the membrane protein H^+ -ATPase, the cytoplasmic isoform of UDP-glucose pyrophosphorylase (UGPase) or the mitochondrial alternative oxidases isoforms (AOX1/2). Anti-GFP antibody was used to detect YFP-RopGEF2.

(b) Coexpression of RopGEF2 with ROPs enhanced the stability of RopGEF2 protein. Five-day-old *YFP-RopGEF2 CFP-ROP* seedlings (crossed hybrid lines), which were treated with $10 \mu\text{M}$ ABA for the indicated times, were analysed by immunoblotting. RopGEF2 protein was detected with anti-GFP antibody. Coomassie staining of the Rubisco large subunit served as a loading control. The arrowhead and asterisk indicate the YFP-RopGEF2 and CFP-ROP bands, respectively.

understood. The evidence presented in this study indicates that RopGEF2 plays a negative role in ABA signalling. The ABA-triggered degradation of RopGEF2 through the ubiquitin-26S proteasome system is required to overcome ABA suppression. The stability of the RopGEF2 protein is associated with its cellular localization and its interaction with ROPs. The binding of RopGEF2 to its target ROPs may ultimately prevent RopGEF2 from being degraded during the response to ABA. The interaction of RopGEF2 and ROP may also alleviate the inactivation of ROPs in response to ABA treatment. The dual mitochondrial and cytosolic localizations of RopGEF2 reveal previously unappreciated connections between RopGEFs and ROPs at mitochondria.

RopGEF2 plays a negative role in the ABA-mediated suppression of seed germination and post-germination growth

Numerous studies have demonstrated the negative roles of ROPs in ABA signalling (Lemichez *et al.*, 2001; Li *et al.*, 2001; Zheng *et al.*, 2002; Yu *et al.*, 2012). For instance, the dominant-negative mutant *DN-rop2* shows hypersensitivity to ABA in seed germination (Li *et al.*, 2001). Similarly, guard cells in *DN-rop6/AtRac1* plants are hypersensitive to ABA (Lemichez *et al.*, 2001). The loss-of-function mutant *rop10-1* shows enhanced ABA sensitivity in various aspects such as root elongation, seed germination and guard cell movement (Zheng *et al.*, 2002). Regulated by FER receptor kinase and three RopGEFs (RopGEF1, RopGEF4 and

RopGEF10), ROP11 can physically interact with phosphatase 2C ABI2 (the negative regulator of ABA signalling) and in turn enhance ABI2 activity, thereby connecting the negative regulation of ABA signalling with ROP activity (Yu *et al.*, 2012). Hence, ROPs may play negative roles in the ABA signal transduction pathway in *Arabidopsis*. In this study, we report that the loss of RopGEF2 function leads to enhanced ABA sensitivity during seed germination and post-germination growth, as demonstrated in the *ropgef2-ko* mutant and in *amiR-RopGEF2* lines. Compared with the WT and the rescued (*Com*) lines, a significant delay in radicle emergence and cotyledon greening was observed in the *ropgef2-ko* and *amiR-RopGEF2* lines (Figures 1, 2 and S1). The specific expression of RopGEF2pro-GUS in developing embryos and germinating seeds (Figure 3) evidently favours the function of RopGEF2 during these two processes. The results of this study demonstrated the necessity of RopGEF2 for overcoming the ABA-mediated inhibition of seed germination and post-germination growth. Further studies into the link between ABA-stimulated ROP inactivation and RopGEF2 function will shed light on the negative regulation of ROP signalling in the ABA response.

Distinct cellular localizations of RopGEF2 may imply its functional divergence

In *Arabidopsis*, 14 members of the RopGEF family (from RopGEF1 to RopGEF14) contain the plant-specific PRONE

domain (Berken *et al.*, 2005; Gu *et al.*, 2006). Several RopGEFs have been reported to localize at the plasma membrane, where they stimulate ROP activity by promoting the exchange of GDP to GTP in ROPs (Gu *et al.*, 2006; Zhang and McCormick, 2007; Chen *et al.*, 2011). Overexpressing *RopGEF1* in tobacco pollen induces the depolarization of pollen tube growth, and the PRONE1 (DUF315) domain is found to be necessary and sufficient for ROP1 activation (Gu *et al.*, 2006). RopGEF12 performs its role in a distinct manner. In pollen tubes, RopGEF12 can collaborate with At-PRK2a at the cell cortex near the plasma membrane to activate the polar growth of pollen tubes (Zhang and McCormick, 2007). RopGEF4 plays a role in the initiation of cell wall patterning. The catalytic PRONE4 domain is localized to the plasma membrane near the secondary cell wall pits, which assemble into a punctuated structure. RopGEF4 is able to antagonize RopGAP3 function at the plasma membrane and regulate the local activation of ROP11 to initiate a distinct pattern of secondary cell walls in xylem cells (Oda and Fukuda, 2012). SPK1, the unique DOCK180-family RopGEF in *Arabidopsis*, is localized at the endoplasmic reticulum sub-domains and is an important player in the early secretory pathway (Zhang *et al.*, 2010). In the present study, we show that RopGEF2 is detectable in the cytoplasm and at mitochondria (Figure 4a–d). The mitochondrial localization of RhoGEFs has not been reported in previous studies, even in mammalian cells. Given the lack of a conserved mitochondrial targeting signal (MTS) in RopGEF2, it is possible that the anchoring of RopGEF2 to the mitochondria is mediated by intermediate components (e.g. scaffold proteins). In mammalian cells, binding to interaction partners or scaffold proteins is essential for the specificity of RhoGEF-regulated Rho GTPase signalling (Marinissen and Gutkind, 2005). In plant cells, the involvement of scaffold proteins in controlling RopGEF-ROP activity or specificity is not well understood. Although RopGEF3, which includes the PRONE3 domain, shares the highest sequence homology with RopGEF2, it does not display mitochondrial localization (Figure S2c). Thus, the mitochondrial localization of RopGEF2 may reflect its unique function in *Arabidopsis*. Moreover, the PRONE2 domain is not sufficient to rescue the cotyledon-greening phenotype of *ropgef2-ko* (Figure S4), implying the need for the N-terminus of RopGEF2 for complete RopGEF2 function.

The departure of RopGEF2 from mitochondria may be achieved when it is bound by ROPs (Figures 5b,d and S3). The fact that translocation of RopGEF2 is possible upon interaction with its targeting ROPs strongly supports this hypothesis. This characteristic of RopGEF2 might imply a regulatory mechanism for cycling ROP signalling in the cell. In fact, such a regulatory mechanism has been reported in mammalian cells (Matsuzawa *et al.*, 2004). When GEF-H1 binds to microtubules at the cell cortex it is

inactive. However, the depolymerization of microtubules allows the departure and activation of GEF-H1. Activated GEF-H1 then promotes the binding of GTP to RhoA. Consequently, myosin II contractility, stress fibre assembly and SRE-regulated gene expression are achieved. Obviously, the redistribution of GEF-H1 is associated with the activation of RhoA in mammalian cells in response to specific stimuli (Matsuzawa *et al.*, 2004). Thus, the dynamic cellular localization of GEFs may be a common mechanism for modulating the spatio-temporal activity of Rho GTPases in either mammalian cells or plant cells responding to environmental signals. The experimental evidence in this report may improve the canonical model of the ROP pathway. Future in-depth studies to depict the spatio-temporal regulation of RopGEF2 in regulating ROP activity will extend our understanding of this aspect.

The ABA-induced degradation of RopGEF2 may occur in the cytosol and ROP binding enhances RopGEF2 stability

Ubiquitination is a three-step process that results in the attachment of ubiquitin, a 76-amino-acid protein, to the lysine residues of substrate proteins, which subsequently leads to the degradation of target proteins via the ubiquitin-26S proteasome system (Smalle and Vierstra, 2004). In mammalian cells, ubiquitination has been implicated as a new layer of regulation for Rho GTPases and their modulators (Nethe and Hordijk, 2010; Ding *et al.*, 2011). The first evidence pinning down the regulation of Rho GTPases by ubiquitination indicated that the ubiquitination and proteasome-mediated degradation of Rac1 can be induced by the bacterial toxin CNF1 (cytotoxic necrotizing factor type 1) (Doye *et al.*, 2002). Thereafter, a number of studies demonstrated the importance of ubiquitination in Rho GTPase-modulated cell mobility (Wang *et al.*, 2003; Nethe and Hordijk, 2010). The modulation of RhoGDI and RhoGEF activity by ubiquitination has also been reported in mammalian cells (Ding *et al.*, 2011). The ubiquitin-26S proteasome system is present in plants and plays a critical role in regulating phytohormone signalling, photomorphogenesis and defence responses in plant cells (Dreher and Callis, 2007; Stone and Callis, 2007; Vierstra, 2009; Santner and Estelle, 2010; Guerra and Callis, 2012; Kelley and Estelle, 2012). However, the role of ubiquitination in modulating the activities of RopGEFs in plant cells has not been reported. In this study, we found that in response to ABA the RopGEF2 protein was degraded via the ubiquitin-26S proteasome system (Figure 6b,f). The pronounced degradation of RopGEF2 was observed in the cytosolic fraction (Figure 7). Hence, decreased levels of RopGEF2 protein in the cytosol might be one of the strategies employed by plant cells to interrupt ROP activity during the response to ABA in *Arabidopsis*. In guard cells, inactivation of *ROP6/AtRac1* can be stimulated by ABA within several minutes (Lemichez *et al.*, 2001). However, the ABA-induced degra-

dation of RopGEF2 in young seedlings is a relatively slow process that takes 120 min (Figure 6). It is likely that the degradation of RopGEF2 protein in the cytosol is not the sole approach to modulating ROP activity. Other regulators such as RhoGAPs and/or RhoGDIs might act in a synergistic manner to control ROP activity. Nevertheless, degradation of RopGEF2 may eventually accelerate the interruption of ROP activation in the presence of ABA.

It is likely that the stability of RopGEF2 is dependent on its state and/or distribution in the cell. When RopGEF2 binds to its target ROPs, it translocates along with ROPs to the cell periphery; hence, the speckled mitochondrial localization of RopGEF2 is diminished (Figures 5b,d and S3). Moreover, when RopGEF2 is bound by ROPs (such as ROP2, ROP6 or ROP10), ABA-induced degradation of RopGEF2 is prevented (Figure 7b). These observations lead to a model in which ROP binding not only alters the localization of RopGEF2 but also stabilizes RopGEF2 protein in the cell. In contrast, if RopGEF2 protein is present in the cytosol in a dissociated form, or not bound by ROPs, it might be easily targeted by a regulatory mechanism such as the ubiquitin-26S proteasome. In the presence of ABA, cytosolic RopGEF2 protein was in fact degraded via the ubiquitin-26S proteasome pathway (Figure 7a). This phenomenon suggests that in response to ABA, RopGEF2 may be degraded in the cytosol through the ubiquitin-26S proteasome system to terminate or inactivate ROP signalling. On the other hand, ABA also induces the accumulation of the GDP form of ROPs in the cytosol (Lemichiez *et al.*, 2001). GDP-bound ROPs are believed to have a higher affinity for RopGEFs (Berken *et al.*, 2005; Rossmann *et al.*, 2005; Basu *et al.*, 2008; Berken and Wittinghofer, 2008). In the cytoplasm, GDP-bound ROPs might in turn bind RopGEF2, forming a feedback loop to prevent degradation of RopGEF2. As such, the ABA-induced deactivation of ROP signalling could be limited.

In summary, RopGEF2 is involved in the ABA-mediated suppression of seed germination and post-germination growth. Based on our results, we propose that RopGEF2 is localized to mitochondria and that ABA can promote the degradation of RopGEF2 protein in the cytosol through the ubiquitin-26S proteasome pathway. The binding of RopGEF2 by ROPs not only alters the localization of RopGEF2 but also prevents its degradation. Hence, the results described in this study raise several questions for future work. In particular, identifying the E3 ligases and/or intermediates responsible for regulating the activity of RopGEF2 protein will strengthen our understanding of the negative regulation of ABA by the ROP signalling pathway. Determining the spatio-temporal correlation between the cellular localization and functional specificity of RopGEF2 will also help elucidate the mechanism of ABA-regulated RopGEF2-ROP activity in plant cells.

EXPERIMENTAL PROCEDURES

Plant materials and growth conditions

All *Arabidopsis* plants were of the Columbia-0 (Col-0) ecotype. The *ropgef2-ko* (SALK_130229) mutant was obtained from the Arabidopsis Biological Resource Center (<http://www.arabidopsis.org/abrc>), and homozygous lines were identified using the protocol described by Alonso *et al.* (2003). Plants were grown in a growth room in 16-h light/8-h dark at 23°C. Information on the plasmids and transgenic lines is provided in Methods S1 and Tables S1 and S2.

Seed germination and seedling growth

Only seeds with the same storage periods were used for the seed germination assay. Surface-sterilized seeds were first sown on Murashige and Skoog (MS) (PhytoTechnology, <http://phytotechlab.com/>) plates containing 1% sucrose and 0.8% (w/v) agar. After 2 days of stratification at 4°C in the dark, the seeds were transferred to a growth chamber. For ABA treatment, sterilized seeds were sown on MS plates containing various concentrations of ABA [(±)-abscisic acid; Sigma-Aldrich, <http://www.sigmaaldrich.com/>]. Control plates contained an equal amount of 100% ethanol, which was used to prepare the ABA stock solution. Radicle emergence and cotyledon greening were then analysed.

Analysis of expression levels using quantitative reverse transcription-PCR

Quantitative reverse transcription-PCR (qRT-PCR) experiments were performed to analyse the expression of *RopGEF2* and *RopGEF3*. To determine the expression levels of *RopGEF2* and *RopGEF3* in the *amiR-RopGEF2* lines, total RNA was isolated from 2-day-old seedlings from WT (Col-0), *ropgef2-ko* and *amiR-RopGEF2* transgenic lines. To examine the expression levels of *RopGEF2* in various *Arabidopsis* tissues, the tested tissues were treated with or without ABA (10 μM) for 24 h. The RNeasy Pure Plant kit (TIANGEN, <http://www.tiangen.com/en/>) was used for RNA isolation. The RNA samples were reverse-transcribed using the ReverTra Ace-α[®] kit (TOYOBO, <http://www.toyobo-global.com/>). Complementary DNA was amplified using the SsoAdvanced SYBR Green supermix (Bio-Rad, <http://www.bio-rad.com/>) with a CFX connect real-time PCR detection system (Bio-Rad). Information on the primers used for qRT-PCR analysis can be found in Table S2.

Purification of cellular fractions and the crude mitochondrial fraction

Membrane and cytosol fractions were prepared through high-speed centrifugation (100 000 g) following a previously described protocol (Lavy *et al.*, 2002). The crude mitochondrial fraction was extracted from protoplasts using the published protocol (Zhong *et al.*, 2008; Møller and Rasmussen, 2013) with some modifications. First, purified protoplasts were re-suspended in lysis buffer [0.3 M sucrose, 60 mM 2-amino-2-(hydroxymethyl)-1,3-propanediol (TRIS)-HCl, pH 7.5, 2 mM EDTA, 10 mM KH₂PO₄, 25 mM tetrasodium pyrophosphate, 1 mM glycine, 1% polyvinylpyrrolidone (PVP), 1% BSA, 50 mM sodium ascorbate]. Then, the lysate was centrifuged (3000 g) for 10 min, and the pellet, which contained cellular debris such as cell wall fragments, starch grains, nuclei and intact chloroplasts, was discarded. The supernatant was centrifuged (10 000 g) for 20 min, and the pellet corresponding to the crude mitochondrial fraction was collected, washed three times with washing buffer (0.3 M sucrose, 10 mM TRIS-HCl, pH 7.5, 2 mM

EDTA, 10 mM KH₂PO₄, 1% PVP, 1% BSA). At the final step, the collected fractions, including membranes, cytosol and mitochondria, were subjected to 10% SDS-PAGE for immunoblotting analysis. The antibodies used for analysis were anti-GFP (Proteintech Group, <http://www.ptglab.com/>), anti-H⁺-ATPase (Agrisera AB, <http://www.agrisera.com/>), anti-UGPase (Agrisera AB) and anti-AOX1/2 (Agrisera AB).

Transient expression assays and microscopic observations

Mesophyll protoplasts were isolated and transformed by following a previously described protocol (Yoo *et al.*, 2007). All plasmid DNAs were purified with caesium chloride-ethidium bromide (CsCl/EB). Three replicates were carried out for each experiment. To analyse the altered localization of RopGEF2 upon ROP binding, plasmids p35S-CFP-ROP2, p35S-CFP-ROP6 or p35S-CFP-ROP10 (4 µg per plasmid) were transformed into mesophyll protoplasts isolated from 5-day-old seedlings from *YFP-RopGEF2* transgenic lines. The transformed protoplasts were incubated for 12 h at 23°C in the dark.

Bombardment was performed by using the PDS-1000/He particle gun delivery system (Bio-Rad), and observations were carried out 12 h after transformation. For the bimolecular fluorescence complementation (BiFC) experiment, plasmids pROP2-YC, pROP6-YC and pROP10-YC (2 µg per plasmid) were each delivered, together with pRopGEF2-YN (2 µg), into the cotyledons of 5-day-old seedlings. To analyse the localization of PRONE2, plasmid p35S-YFP-PRONE2 (8 µg) was delivered into the epidermal cells of *Arabidopsis* roots and leaves or onion peels. To analyse the colocalization of ROPs and PRONE2, plasmids p35S-YFP-PRONE2 (8 µg) and p35S-CFP-ROP2 (4 µg), or p35S-CFP-ROP6 (4 µg) or p35S-CFP-ROP10 (4 µg) were delivered into the epidermal cells of onion peels.

To observe the Mito Tracker Red signal, protoplasts were isolated from the 5-day-old *YFP-RopGEF2* transgenic seedlings. Purified protoplasts were incubated with 50 nM Mito Tracker Red CMXRos (Invitrogen, <http://www.invitrogen.com/>) for 15 min at 25°C. The stained protoplasts were then subjected to microscopic observation. The fluorescent signal of Mito Tracker Red was acquired at 579 nm (excitation) and 599 nm (emission); YFP fluorescence was visualized at 515 nm (excitation) and 535 nm (emission); CFP fluorescence was visualized at 440 nm (excitation) and 480 nm (emission); DsRed fluorescence was observed at 550 nm (excitation) and 585 nm (emission); FITC fluorescence was visualized at 492 nm (excitation) and 520 nm (emission); and Cy3 fluorescence was observed at 550 nm (excitation) and 570 nm (emission). All images were acquired on an Olympus Confocal Laser Scanning Microscope FV1000 (Olympus, <http://www.olympus.com/>).

Pull-down assays

Pull-down assays were carried out following a previously described protocol, with some modifications (Gu *et al.*, 2006; Wu *et al.*, 2013). His-ROP proteins (10 µg each) were incubated with GST-RopGEF2 protein (50 µg), which was conjugated to glutathione sepharose beads (GE Healthcare, <http://www3.gehealthcare.com/>) in 500 µl of binding buffer (20 mM TRIS-HCl, pH 7.5, 150 mM NaCl, 10% glycerol, 0.1% Triton X-100, 5 mM MgCl₂, 1 mM EDTA), for 1 h at 4°C. Then, the beads were washed five times with binding buffer to remove unbound proteins. The protein complex was separated by 10% SDS-PAGE and blotted with anti-His antibody (Proteintech Group).

For semi-*in-vivo* pull-down of RopGEF2 and ROP2, ROP6 or ROP10, the purified His-ROP2, His-ROP6 and His-ROP10 proteins

(20 µg per sample) were first conjugated to TALON beads. Then, TALON bead-bound His-ROP2, His-ROP6 or His-ROP10 was incubated for 1 h at 4°C with total protein that was extracted from 5-day-old *YFP-RopGEF2* transgenic seedlings. The beads were washed five times. At the last step, the precipitated protein complex was separated via 10% SDS-PAGE and analysed using an anti-GFP antibody (Proteintech Group).

RopGEF2 degradation assay and ubiquitination assay

For the degradation assay, 5-day-old *YFP-RopGEF2* transgenic seedlings were pre-treated with MG132 (50 µM) for 2 h and then treated with ABA (10 µM) for the indicated times. Afterwards, total proteins were prepared in extraction buffer [25 mM TRIS-HCl, pH 7.5, 150 mM NaCl, 2 mM DTT, 1 mM NaF, 0.5 mM Na₃VO₄, 15 mM β-glycerophosphate, 0.5 mM phenylmethylsulfonyl fluoride (PMSF) and protease inhibitor cocktail]. Equal amounts of protein samples from each treatment were analysed by immunoblotting with anti-GFP antibody (Proteintech Group).

For the ubiquitination assay, we followed a previously described protocol (Liu and Stone, 2010), with minor modifications. Total protein extracts were prepared from 5-day-old *YFP-RopGEF2* transgenic seedlings that were treated with or without ABA (10 µM). To remove unbound non-specific proteins, Protein A+G Agarose beads (Beyotime, <http://www.beyotime.com/>) were incubated with protein samples for 1 h at 4°C. After a brief centrifugation (500 g, 10 s), the supernatant was collected and incubated with anti-GFP antibody for 16 h at 4°C. Next, the protein mixture was incubated with Protein A+G Agarose beads for 2 h at 4°C. After centrifugation (500 g) for 5 min, the beads were washed five times with washing buffer. Finally, the immunoprecipitated protein pellets were denatured and analysed by immunoblotting using anti-GFP and anti-ubiquitin antibodies (Sigma). Expression of *YFP-RopGEF2* protein was examined by immunoblotting using anti-GFP antibody. Transgenic seedlings expressing GFP alone were used as the control.

ACKNOWLEDGEMENTS

We thank the members of the Wu Lab for their technical help and helpful comments on the manuscript. We thank Dr Nam-Hai Chua (Rockefeller University, USA) for providing plasmid pBA002. We thank the 'Large-scale Instrument and Equipment Sharing Foundation of Wuhan University' for supporting the use of the instruments in the College of Life Sciences in Wuhan University. This work was supported by grants to YW from the National Natural Science Foundation of China (31270333 and 90817013), the Major State Basic Research Program from the Ministry of Science and Technology of China (2013CB126900) and the Chinese 111 Project (B06018).

SUPPORTING INFORMATION

Additional Supporting Information may be found in the online version of this article.

Figure S1. The *amiR-RopGEF2* lines showed enhanced sensitivity to ABA treatments.

Figure S2. Analysis of transgenic plants expressing *YFP-RopGEF2* and assessment of the cellular localization of YFP-RopGEF3 and YFP-PRONE3.

Figure S3. Co-expressing *YFP-RopGEF2* with ROPs altered its mitochondrial localization.

Figure S4. *PRONE2* overexpression could not rescue the cotyledon-greening phenotype in *ropgef2-ko* seedlings.

Table S1. Plasmids used in this study.

Table S2. Primer sequences used for plasmid construction and in analysing *RopGEFs* and *ROP* expression levels.

Methods S1. Supporting materials and methods.

REFERENCES

- Alonso, J.M., Stepanova, A.N., Leisse, T.J. et al. (2003) Genome-wide insertional mutagenesis of *Arabidopsis thaliana*. *Science*, **301**, 653–657.
- Basu, D., Le, J., Zakharova, T., Mallery, E.L. and Szymanski, D.B. (2008) A SPIKE1 signaling complex controls actin-dependent cell morphogenesis through the heteromeric WAVE and ARP2/3 complexes. *Proc. Natl Acad. Sci. USA*, **105**, 4044–4049.
- Berken, A. (2006) ROPs in the spotlight of plant signal transduction. *Cell. Mol. Life Sci.* **63**, 2446–2459.
- Berken, A. and Wittinghofer, A. (2008) Structure and function of Rho-type molecular switches in plants. *Plant Physiol. Biochem.* **46**, 380–393.
- Berken, A., Thomas, C. and Wittinghofer, A. (2005) A new family of Rho-GEFs activates the Rop molecular switch in plants. *Nature*, **436**, 1176–1180.
- Chang, F., Gu, Y., Ma, H. and Yang, Z. (2013) AtPRK2 promotes ROP1 activation via RopGEFs in the control of polarized pollen tube growth. *Mol. Plant*, **6**, 1187–1201.
- Chen, M., Liu, H.L., Kong, J.X. et al. (2011) RopGEF7 regulates PLETHORA-dependent maintenance of the root stem cell niche in *Arabidopsis*. *Plant Cell*, **23**, 2880–2894.
- Côté, J.F. and Vuori, K. (2007) GEF what? Dock180 and related proteins help Rac to polarize cells in new ways. *Trends Cell Biol.* **17**, 383–393.
- Craddock, C., Lavagi, I. and Yang, Z. (2012) New insights into Rho signaling from plant ROP/Rac GTPases. *Trends Cell Biol.* **22**, 492–501.
- Cutler, S.R., Rodriguez, P.L., Finkelstein, R.R. and Abrams, S.R. (2010) Abscisic acid: emergence of a core signaling network. *Annu. Rev. Plant Biol.* **61**, 651–679.
- Ding, F., Yin, Z. and Wang, H.R. (2011) Ubiquitination in Rho signaling. *Curr. Top. Med. Chem.* **11**, 2879–2887.
- Doye, A., Mettouchi, A., Bossis, G., Clément, R., Buisson-Touati, C., Flatau, G., Gagnoux, L., Piechaczky, M., Boquet, P. and Lemichez, E. (2002) CNF1 exploits the ubiquitin-proteasome machinery to restrict Rho GTPase activation for bacterial host cell invasion. *Cell*, **111**, 553–564.
- Dreher, K. and Callis, J. (2007) Ubiquitin, hormones and biotic stress in plants. *Ann. Bot.* **99**, 787–822.
- Finkelstein, R.R., Gampala, S.S.L. and Rock, C.D. (2002) Abscisic acid signaling in seeds and seedlings. *Plant Cell*, **14**, S15–S45.
- Fujii, H., Chinnusamy, V., Rodrigues, A., Rubio, S., Antoni, R., Park, S.Y., Cutler, S.R., Sheen, J., Rodriguez, P.L. and Zhu, J.K. (2009) In vitro reconstitution of an abscisic acid signalling pathway. *Nature*, **462**, 660–664.
- Gu, Y., Li, S.D., Lord, E.M. and Yang, Z.B. (2006) Members of a novel class of Arabidopsis Rho guanine nucleotide exchange factors control Rho GTPase-dependent polar growth. *Plant Cell*, **18**, 366–381.
- Guerra, D.D. and Callis, J. (2012) Ubiquitin on the move: the ubiquitin modification system plays diverse roles in the regulation of endoplasmic reticulum- and plasma membrane-localized proteins. *Plant Physiol.* **160**, 56–64.
- Hauser, F., Waadt, R. and Schroeder, J.I. (2011) Evolution of abscisic acid synthesis and signaling mechanisms. *Curr. Biol.* **21**, R346–R355.
- Kelley, D.R. and Estelle, M. (2012) Ubiquitin-mediated control of plant hormone signaling. *Plant Physiol.* **160**, 47–55.
- Kost, B. (2008) Spatial control of Rho (Rac-Rop) signaling in tip-growing plant cells. *Trends Cell Biol.* **18**, 119–127.
- Lavy, M., Bracha-Drori, K., Sternberg, H. and Yalovsky, S. (2002) A cell-specific, prenylation-independent mechanism regulates targeting of type II RACs. *Plant Cell*, **14**, 2431–2450.
- Lemichez, E., Wu, Y., Sanchez, J.P., Mettouchi, A., Mathur, J. and Chua, N.H. (2001) Inactivation of AtRac1 by abscisic acid is essential for stomatal closure. *Genes Dev.* **15**, 1808–1816.
- Li, H., Shen, J.J., Zheng, Z.L., Lin, Y.K. and Yang, Z.B. (2001) The Rop GTPase switch controls multiple developmental processes in *Arabidopsis*. *Plant Physiol.* **126**, 670–684.
- Li, Z., Kang, J., Sui, N. and Liu, D. (2012) ROP11 GTPase is a negative regulator of multiple ABA responses in *Arabidopsis*. *J. Integr. Plant Biol.* **54**, 169–179.
- Liu, H. and Stone, S.L. (2010) Abscisic acid increases Arabidopsis ABI5 transcription factor levels by promoting KEG E3 ligase self-ubiquitination and proteasomal degradation. *Plant Cell*, **22**, 2630–2641.
- Lopez-Molina, L., Mongrand, S. and Chua, N.H. (2001) A postgermination developmental arrest checkpoint is mediated by abscisic acid and requires the ABI5 transcription factor in *Arabidopsis*. *Proc. Natl Acad. Sci. USA*, **98**, 4782–4787.
- Ma, Y., Szostkiewicz, I., Korte, A., Moes, D., Yang, Y., Christmann, A. and Grill, E. (2009) Regulators of PP2C phosphatase activity function as abscisic acid sensors. *Science*, **324**, 1064–1068.
- Marinissen, M.J. and Gutkind, J.S. (2005) Scaffold proteins dictate Rho GTPase-signaling specificity. *Trends Biochem. Sci.* **30**, 423–426.
- Matsuzawa, T., Kuwae, A., Yoshida, S., Sasakawa, C. and Abe, A. (2004) Enteropathogenic *Escherichia coli* activates the RhoA signaling pathway via the stimulation of GEF-H1. *EMBO J.* **23**, 3570–3582.
- Miyakawa, T., Fujita, Y., Yamaguchi-Shinozaki, K. and Tanokura, M. (2013) Structure and function of abscisic acid receptors. *Trends Plant Sci.* **18**, 259–266.
- Møller, I.M. and Rasmussen, A.G. (2013) Topic 12.1: Isolation of Mitochondria. Plant Physiology and Development, Sixth Edition online. <http://6e.plantphys.net/topic12.01.html>. (accessed October 2015).
- Nethe, M. and Hordijk, P.L. (2010) The role of ubiquitylation and degradation in RhoGTPase signalling. *J. Cell Sci.* **123**, 4011–4018.
- Oda, Y. and Fukuda, H. (2012) Initiation of cell wall pattern by a Rho- and microtubule-driven symmetry breaking. *Science*, **337**, 1333–1336.
- Park, S.Y., Fung, P., Nishimura, N. et al. (2009) Abscisic acid inhibits type 2C protein phosphatases via the PYR/PYL family of START proteins. *Science*, **324**, 1068–1071.
- Qiu, J.L., Jilk, R., Marks, M.D. and Szymanski, D.B. (2002) The *Arabidopsis* SPIKE1 gene is required for normal cell shape control and tissue development. *Plant Cell*, **14**, 101–118.
- Raghavendra, A.S., Gonugunta, V.K., Christmann, A. and Grill, E. (2010) ABA perception and signalling. *Trends Plant Sci.* **15**, 395–401.
- Rossmann, K.L., Der, C.J. and Sonddek, J. (2005) GEF means go: turning on RHO GTPases with guanine nucleotide-exchange factors. *Nat. Rev. Mol. Cell Biol.* **6**, 167–180.
- Santner, A. and Estelle, M. (2010) The ubiquitin-proteasome system regulates plant hormone signaling. *Plant J.* **61**, 1029–1040.
- Shichur, K. and Yalovsky, S. (2006) Turning ON the switch-RhoGEFs in plants. *Trends Plant Sci.* **11**, 57–59.
- Smalle, J. and Vierstra, R.D. (2004) The ubiquitin 26S proteasome proteolytic pathway. *Annu. Rev. Plant Biol.* **55**, 555–590.
- Stone, S.L. and Callis, J. (2007) Ubiquitin ligases mediate growth and development by promoting protein death. *Curr. Opin. Plant Biol.* **10**, 624–632.
- Vierstra, R.D. (2009) The ubiquitin-26S proteasome system at the nexus of plant biology. *Nat. Rev. Mol. Cell Biol.* **10**, 385–397.
- Wang, H.R., Zhang, Y., Ozdamar, B., Ogunjimi, A.A., Alexandrova, E., Thomsen, G.H. and Wrana, J.L. (2003) Regulation of cell polarity and protrusion formation by targeting RhoA for degradation. *Science*, **302**, 1775–1779.
- Wang, Y., Li, L., Ye, T., Zhao, S., Liu, Z., Feng, Y.Q. and Wu, Y. (2011) Cytokinin antagonizes ABA suppression to seed germination of *Arabidopsis* by downregulating ABI5 expression. *Plant J.* **68**, 249–261.
- Wang, Y., Li, L., Ye, T., Lu, Y., Chen, X. and Wu, Y. (2013) The inhibitory effect of ABA on floral transition is mediated by ABI5 in *Arabidopsis*. *J. Exp. Bot.* **64**, 675–684.
- Wu, H.M., Hazak, O., Cheung, A.Y. and Yalovsky, S. (2011) RAC/ROP GTPases and auxin signaling. *Plant Cell*, **23**, 1208–1218.
- Wu, Y., Zhao, S., Tian, H., He, Y., Xiong, W., Guo, L. and Wu, Y. (2013) CPK3-phosphorylated RhoGDI1 is essential in the development of *Arabidopsis* seedlings and leaf epidermal cells. *J. Exp. Bot.* **64**, 3327–3338.
- Yang, Z. (2002) Small GTPases: versatile signaling switches in plants. *Plant Cell*, **14**(Suppl.), S375–S388.
- Yang, Z. (2008) Cell polarity signaling in *Arabidopsis*. *Annu. Rev. Cell Dev. Biol.* **24**, 551–575.
- Yoo, S.D., Cho, Y.H. and Sheen, J. (2007) Arabidopsis mesophyll protoplasts: a versatile cell system for transient gene expression analysis. *Nat. Protoc.* **2**, 1565–1572.
- Yu, F., Qian, L., Nibau, C. et al. (2012) FERONIA receptor kinase pathway suppresses abscisic acid signaling in *Arabidopsis* by activating ABI2 phosphatase. *Proc. Natl Acad. Sci. USA*, **109**, 14693–14698.

- Zhang, Y. and McCormick, S.** (2007) A distinct mechanism regulating a pollen-specific guanine nucleotide exchange factor for the small GTPase Rop in *Arabidopsis thaliana*. *Proc. Natl Acad. Sci. USA*, **104**, 18830–18835.
- Zhang, Y. and McCormick, S.** (2010) The regulation of vesicle trafficking by small GTPases and phospholipids during pollen tube growth. *Sex. Plant Reprod.* **23**, 87–93.
- Zhang, C., Kotchoni, S.O., Samuels, A.L. and Szymanski, D.B.** (2010) SPIKE1 signals originate from and assemble specialized domains of the endoplasmic reticulum. *Curr. Biol.* **20**, 2144–2149.
- Zheng, Z.L., Nafisi, M., Tam, A., Li, H., Crowell, D.N., Chary, S.N., Schroeder, J.I., Shen, J.J. and Yang, Z.B.** (2002) Plasma membrane-associated ROP10 small GTPase is a specific negative regulator of abscisic acid responses in *Arabidopsis*. *Plant Cell*, **14**, 2787–2797.
- Zhong, B., Yang, Y., Li, S. et al.** (2008) The adaptor protein MITA links virus-sensing receptors to IRF3 transcription factor activation. *Immunity*, **29**, 538–550.